

Supporting Information:

Enhancing Self-Assembly in Cellulose
Nanocrystal Suspensions Using High-
Permittivity Low Acidity Solvents

Johanna R. Bruckner^a, Anja Kuhnhold^b, Camila Honorato-Rios^a, Tanja Schilling^b,
Jan P. F. Lagerwall^{a*}

^aExperimental Soft Matter Physics Group, Physics and Materials Science Research Unit,
University of Luxembourg, 162a, Avenue de la Faïencerie, L-1511 Luxembourg, Luxembourg

^bTheoretical Materials' Science Group, Physics and Materials Science Research Unit, University
of Luxembourg, 162a, Avenue de la Faïencerie, L-1511 Luxembourg, Luxembourg

Additional Experimental Details

Measurement of Refractive Indices. To check that the investigated organic solvents and water do not form an azeotrope and can be separated with the solvent exchange method described in the main article, measurements of the refractive indices n_D^{20} were performed. To this end, the organic solvent and water were mixed, followed by evaporation of the water under the same conditions as described for the solvent exchange. The refractive index of the resulting liquid was measured with a refractometer (Anton Paar) at 20°C with a wavelength of 589 nm (sodium D-line). The obtained refractive indices were compared with the literature values (Tab. S1) and showed a good agreement.

Table S1. Refractive indices n_D^{20} of the water/solvent mixtures after removal of the water.

Organic solvent	n_D^{20} (literature value)	n_D^{20} (after separation)
Formamid	1.4472	1.4476
NMF	1.4319	1.4320
DMF	1.4305	1.4307

Establishment of Phase Diagrams. Dilutions for establishing the phase diagram were prepared in vials with a volume of 2 mL. To minimize the formation of a meniscus the vials were silanized with a solution of 1 vol% of trichloro(octadecyl)silane ($\geq 90\%$, Sigma-Aldrich) in toluene (EMSURE[®] ACS, ISO, Reag. Ph Eur, Merck) followed by rinsing with toluene and methanol (Rotisolv[®] HPLC, Carl Roth). The initial CNC suspensions were diluted with deionized water or

the respective purified solvent, the desired fractions of CNC starting suspension and diluent being established using a Sartorius analytical balance. Dilutions for other investigations were prepared in the same way but in untreated glass vials.

To guarantee a good separation of the anisotropic and the isotropic fractions, the CNC suspensions, filled in sealed glass vials, were centrifuged for 30 min at 4000 rpm. For measuring the phase diagrams the vials were placed between crossed polarizers and photographed with a Canon EOS 100D camera (Fig. S1-S4). The volume fraction of the anisotropic phase was determined from these pictures by using the software MB-Ruler.

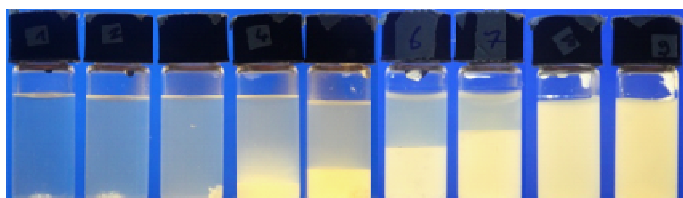


Figure S1. Phase diagram of the CNC/water system from 1 (left-most vial) to 9 wt% (right-most vial), in steps of 1 wt%.

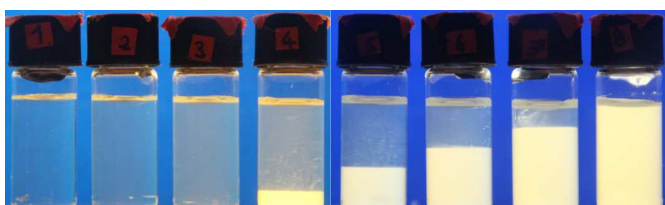


Figure S2. Phase diagram of the CNC/formamide system from 1 (left-most vial) to 8 wt% (right-most vial), in steps of 1 wt%.

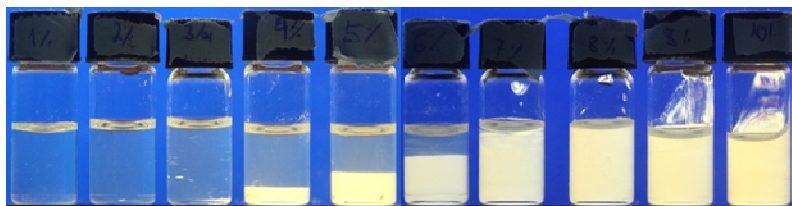


Figure S3. Phase diagram of the CNC/NMF system from 1 (left-most vial) to 10 wt% (right-most vial), in steps of 1 wt%.

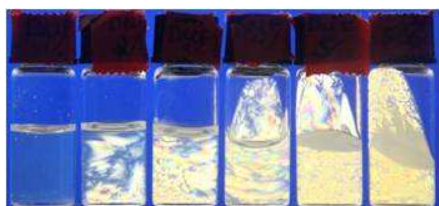


Figure S4. Phase diagram of the CNC/DMF system from 1 (left-most vial) to 6 wt% (right-most vial), in steps of 1 wt%.

To verify that centrifugation of the samples only speeds up the separation of the isotropic and the anisotropic phases and does not change the volume fractions, comparative investigations were made for the CNC/formamide system. For this the same samples were used as in Figure S2, mixed thoroughly until there was no more phase separation and left for equilibration for 3 months. After this time, the samples showed the same degree of phase separation as after centrifugation, as can be seen by comparing Figures S5 and S2.

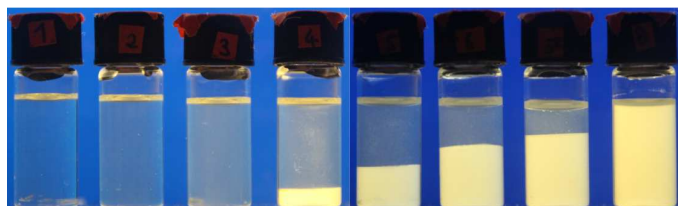


Figure S5. CNC/formamide system from 1 (left-most vial) to 8 wt% (right-most vial), in steps of 1 wt% after 3 months of equilibration.

Atomic Force Microscopy. A 20 μL volume of poly-L-lysine (cationic) solution (0.01 vol.%) was deposited on a freshly cleaved mica (anionic) surface (NanoAn- 45 dMore GMBH) and was allowed to react for 3 min. Subsequently the mica substrate was rinsed with deionized water and dried with compressed air. A 20 μL volume of a CNC (anionic) dispersion (0.0015 wt%) was placed on the treated surface for 3 min, the CNC rods adsorbing on the poly-L-lysine surface due to electrostatic attraction. After rinsing with deionized water the samples were dried with compressed air, followed by drying in a vacuum oven at 30°C overnight. A Multi-mode V AFM (Digital instruments Nanoscope Veeco) was used in tapping mode to image the samples, using AFM probes from Budget Sensors (Tap300 Al-G, resonance frequency 300 kHz and force constant 40 N/m). The AFM image was processed with the software NanoScope Analysis 1.7. From these images (Fig. S6), the length distribution of the CNCs was determined using the software ImageJ.

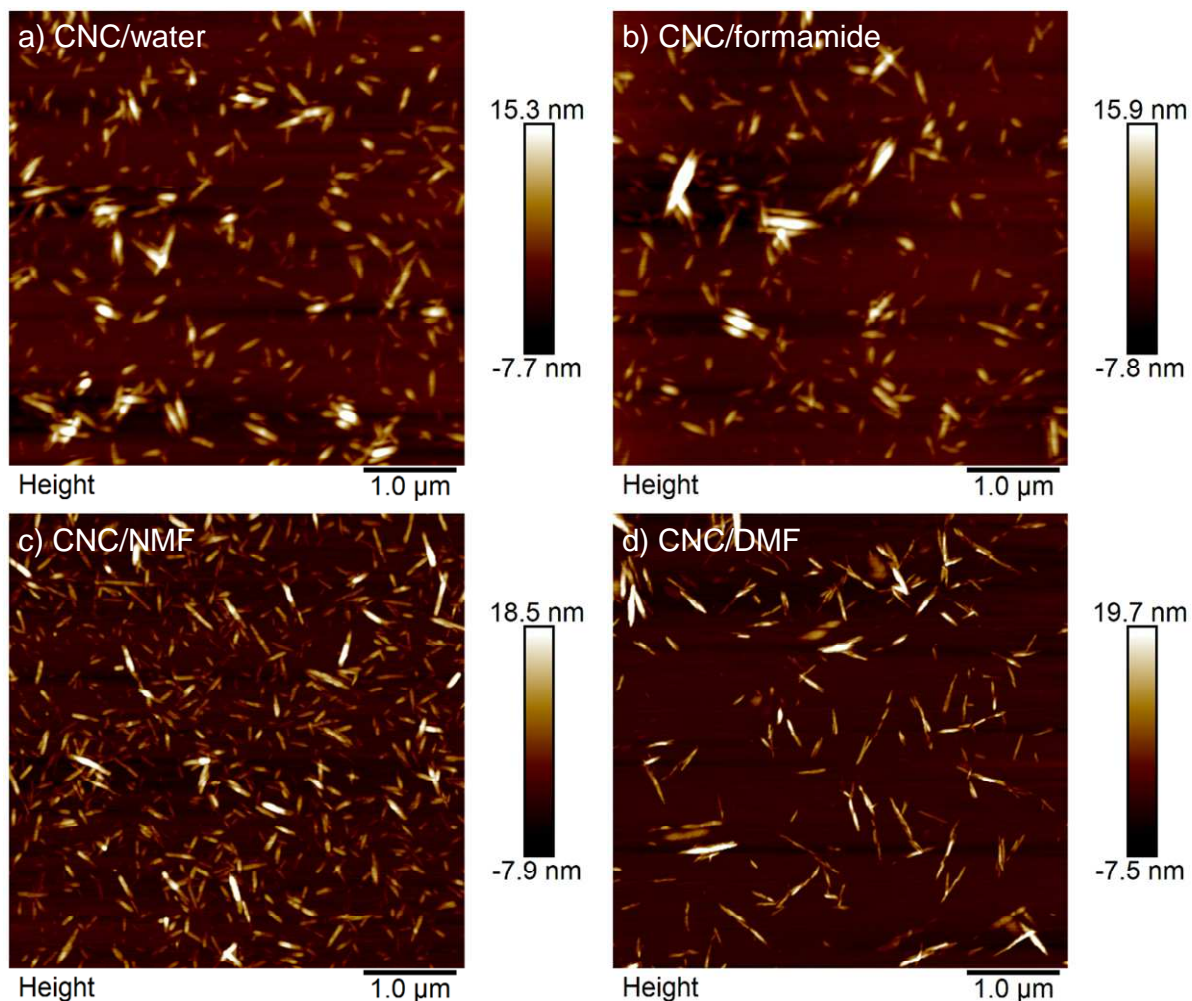


Figure S6. AFM images of CNCs suspended in a) water, b) formamide, c) NMF and d) DMF.

Measurements of the Chiral Nematic Pitch. For measuring the chiral nematic pitch, the CNC suspensions were filled into capillaries with a rectangular cross section and an inner dimension of $0.40 \times 2.00 \text{ mm}^2$ made of borosilicate glass (VitroCom). To avoid the evaporation of solvent, the capillaries were sealed with glue (Pattex). After the glue was dried, the capillaries were left standing upright for 16 to 20 days to allow equilibration. The pitch was then measured using two

different methods. For the ‘direct method’ the capillaries were observed using the polarizing microscope BX51 (Olympus) and images of the texture were taken with an Olympus DP73 digital camera which was controlled by the software cellSens. The helical pitch was determined from these pictures as twice the distance between lines (“pitch lines”) in the characteristic finger print texture by using the software ImageJ. To minimize errors up to 12 pitch lines were considered for measuring the pitch and the measurement was repeated five times at different positions in the sample. The second method used is laser light diffraction. For this the light of a He-Ne laser ($\lambda = 632.8$ nm) was pointed at the capillaries. The laser light which was diffracted at the pitch lines hit a white screen and was photographed using a Canon EOS 100D (ISO 100, $f = 4.0$ mm, exposure time 0.5-5 s). The pictures were analyzed using the software ImageJ with a radial profile plugin (Paul Baggethun). The scattering maxima were determined from the radial profile plots by fitting a Lorentzian function to the data, using the software QtiPlot. To calibrate the variable sample to detector distance a grid with a period of $30 \mu\text{m}$ was used.

Investigation of the Temporal Evolution of the Chiral Nematic Pitch. To investigate the temporal evolution of the chiral nematic pitch, the CNC suspensions were filled into capillaries with a rectangular cross section and an inner dimension of $0.10 \times 2.00 \text{ mm}^2$ made of borosilicate glass (VitroCom) and the filling time was noted. Within less than 10 min after filling, the capillaries were placed in a polarizing microscope (Leitz, Laborlux 12 Pol S) and the temporal evolution of the texture was recorded by taking a picture every 5 min (Fig. S7) with a software controlled ScopeTek DCM500 digital camera. From these pictures the time between filling the

capillaries and the first signs of pitch lines as well as the formation of clearly visible pitch lines were determined.

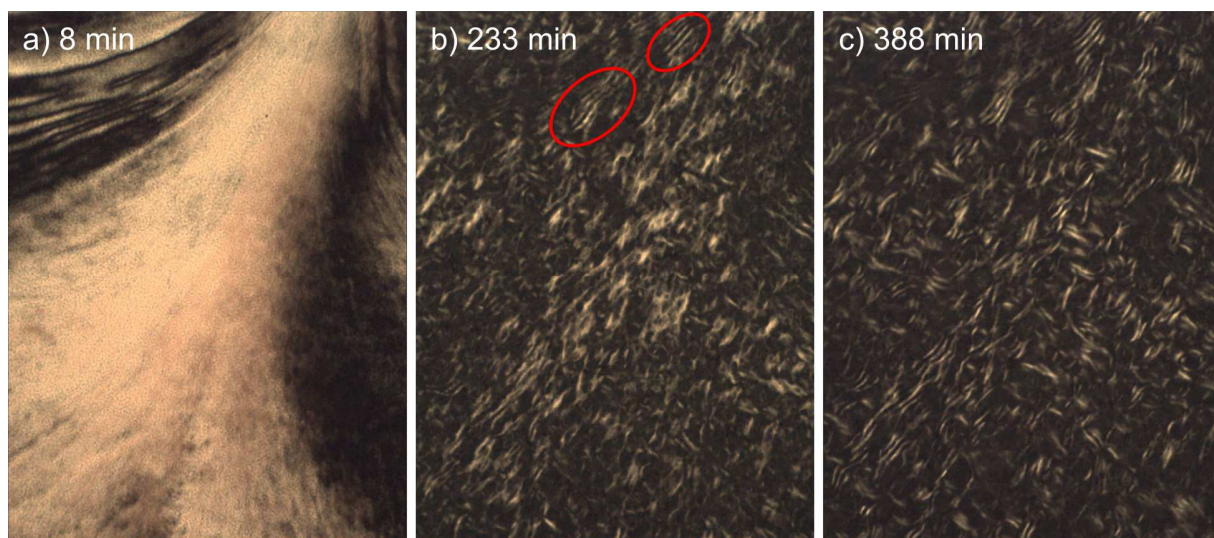


Figure S7. Temporal evolution of the helical structure in a CNC/formamide sample with 7 wt% of CNCs: a) immediately after filling the sample shows a planar texture due to shear forces, b) after 233 min first signs of pitch lines appear in the upper corner of the picture marked with red circles, c) after 388 min clearly visible pitch lines can be found all over the picture.

Rheological Investigations. All accessible mass fractions of the four different CNC suspension types were investigated rheologically using a Haake Mars rotational rheometer (Thermo Electron Cooperation) with a parallel plate geometry of 35 mm diameter. The flow curves (Fig. S8-S11) were measured in a shear range between 0.01 and 100 s⁻¹ for each sample. For highly viscous samples frequency sweep measurements were carried out additionally over an angular frequency range from 0.628 to 62.8 rad s⁻¹ (0.1 to 10 Hz). The linear viscoelastic region was determined beforehand by amplitude sweep experiments. All measurements were performed at room

temperature ($(20 \pm 1)^\circ\text{C}$) and started right after the sample was placed into the rheometer. In case of the CNC suspensions with water as solvent, evaporating comparatively fast, sponges soaked with water were placed around the measurement region to ensure a saturated humidity.

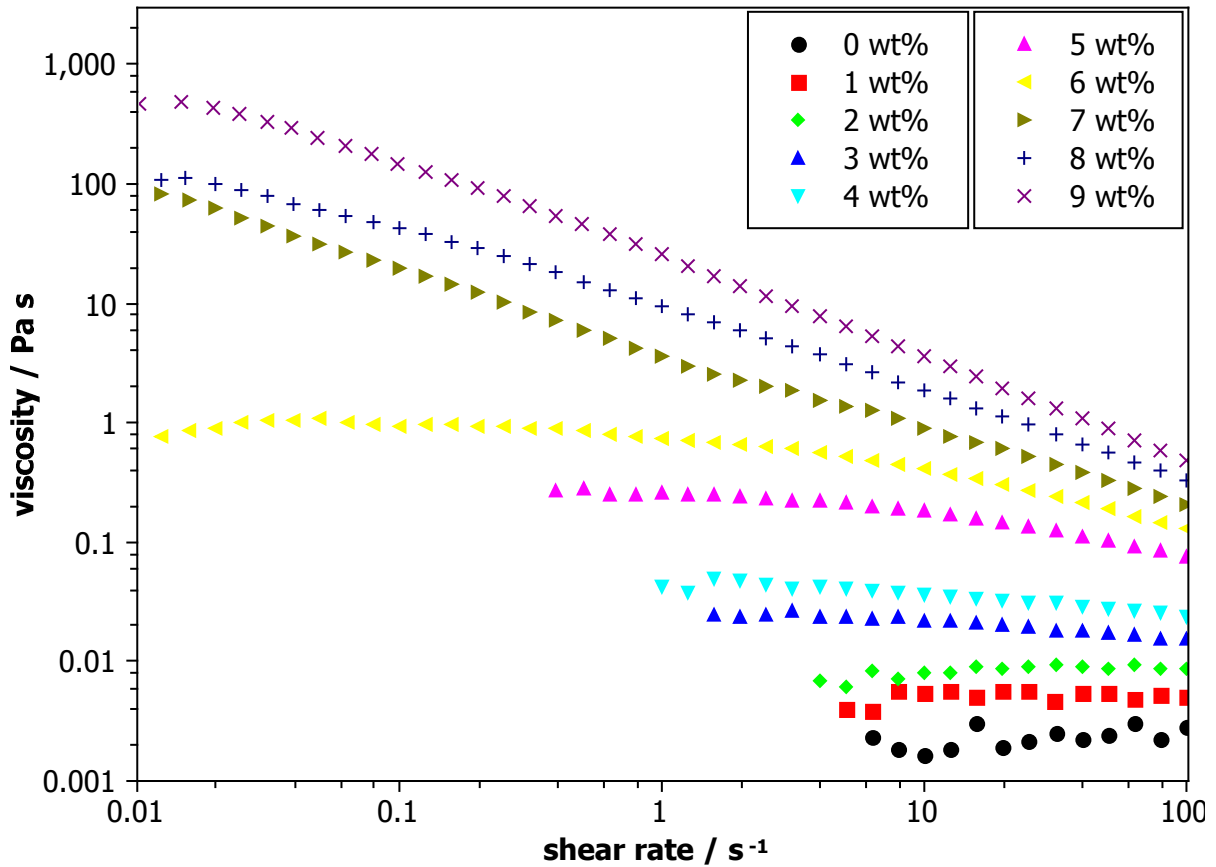


Figure S8. Flow curves measured for CNC suspensions in water from 0 to 9 wt% of CNCs. Already at 7 wt% the viscosity is dramatically increased.

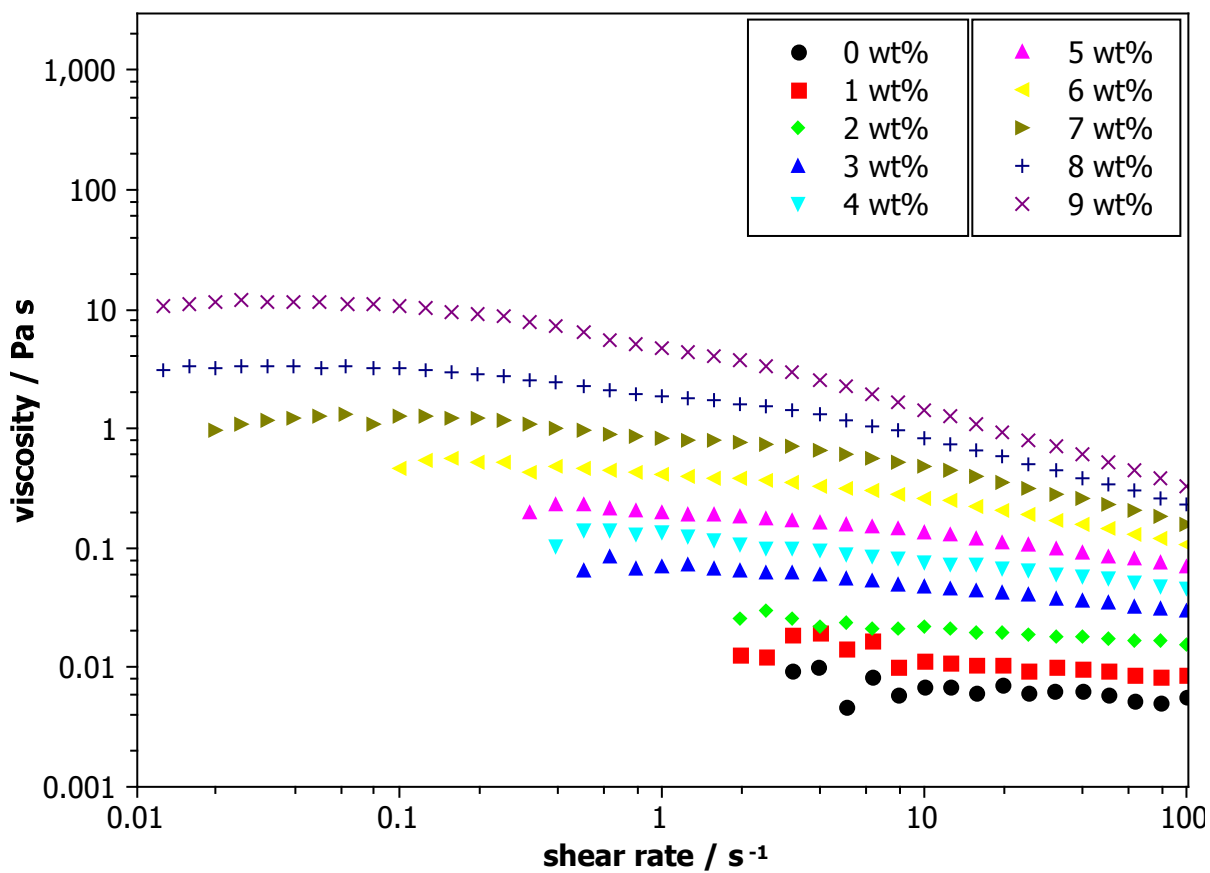


Figure S9. Flow curves measured for CNC suspensions in formamide from 0 to 9 wt% of CNCs. Up to 9 wt% the flow curves still show the three-region behavior typical of ordered fluids.

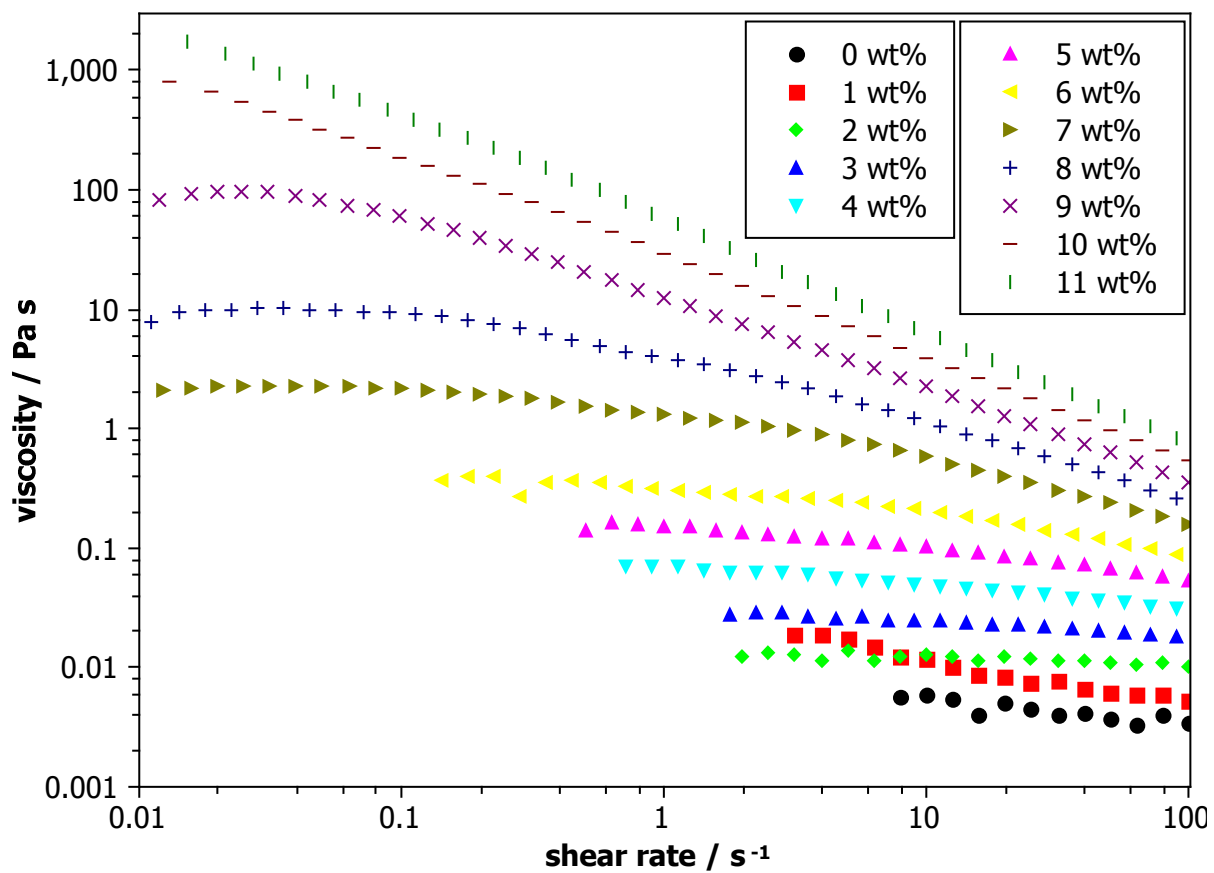


Figure S10. Flow curves measured for CNC suspensions in NMF from 0 to 11 wt% of CNCs.

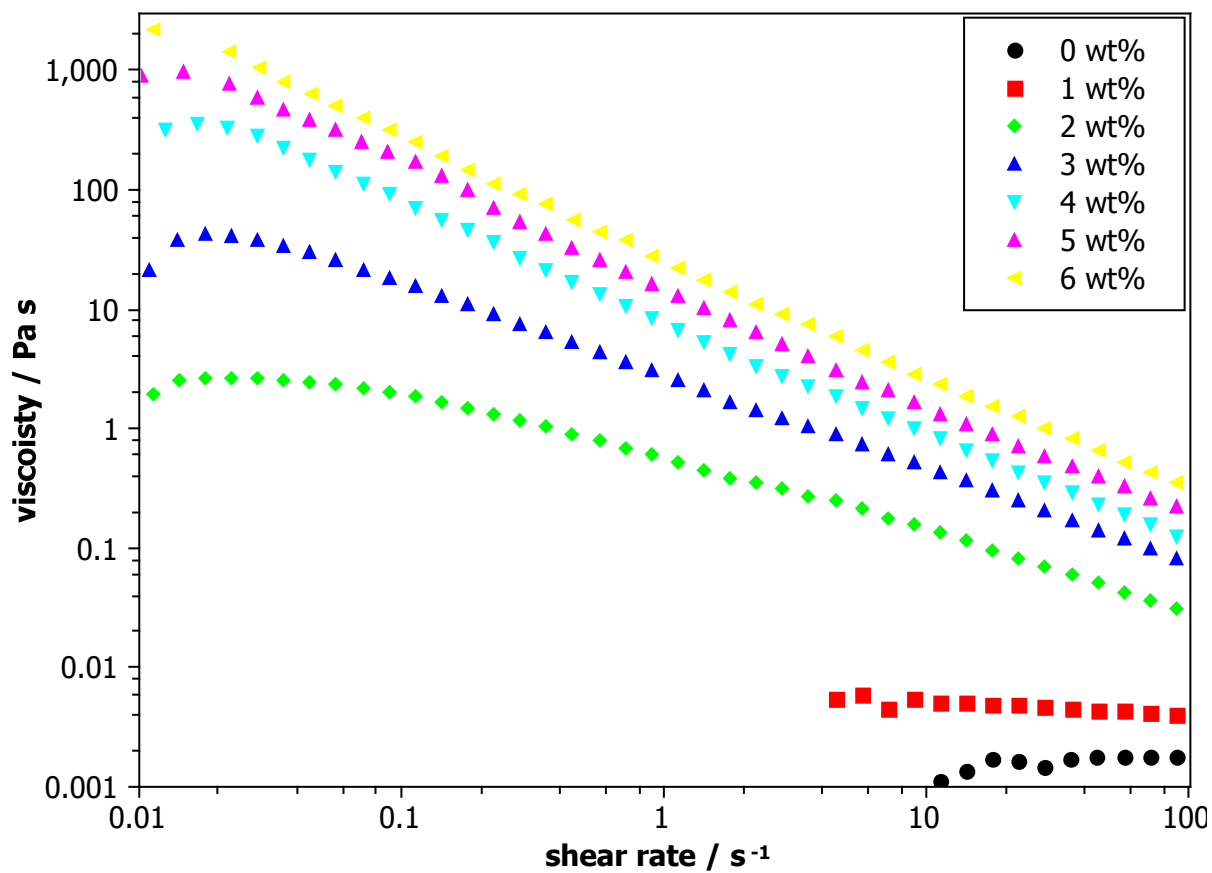


Figure S11. Flow curves measured for CNC suspensions in DMF from 0 to 6 wt% of CNCs. The transition into the arrested state between 1 and 2 wt% is clearly visible.